Clay Minerals (2026), **61**, 239–255
doi:10.1180/clm.2026.10041

Article

Comparative performance of iron-modified natural zeolites for chromium(VI) removal from aqueous solutions

Bruno Freitas Pio de Azevedo[1], Francesco Panattoni[2], Marianna Tardani[2], Natale Perchiazzi[1], Lisa Ghezzi[1] and Enrico Mugnaioli[1]

[1]Dipartimento di Scienze della Terra, Via S. Maria 53, 56126 Pisa, Italy and [2]DND Biotech srl, via S. Cannizzaro 5, 56121 Pisa, Italy

Abstract

Natural zeolites modified with iron(II) ions or iron(III) phases represent two promising approaches for treating hexavalent chromium contamination in water due to their reduction and adsorption capacities, respectively. However, comprehensive comparative analysis of their efficiency remains limited. Fe(II)-modified zeolites can reduce Cr(VI) to the less toxic and insoluble Cr(III) form, while Fe(III)-modified zeolites primarily remove Cr(VI) through surface adsorption. This study evaluates the effectiveness of Fe(II)- and Fe(III)-modified zeolites using synthetic Cr solutions and real contaminated surface water. The materials were characterized *via* X-ray diffraction, scanning electron microscopy, transmission electron microscopy and X-ray fluorescence spectroscopy to assess their chemical, structural and morphological changes before and after chromium sorption. Batch and column tests determined Cr(VI) removal capacity, while Cr isotopes were used to track reduction reactions. The Fe(II) enrichment *via* cation exchange was highly effective. The Fe(II)-modified zeolite demonstrated a greater capacity for Cr(VI) removal from contaminated solutions, primarily through a reduction mechanism that converted Cr(VI) to Cr(III), as was confirmed by isotopic analysis. Its performance improved under higher-salinity conditions. However, it required prolonged contact time with the contaminant to achieve optimal efficiency. The Fe(III)-modified zeolite exhibited a heterogeneous distribution of iron oxide/hydroxide phases on its surface. This material showed some favourable characteristics in batch and column tests, including a notably faster Cr removal rate due to direct Cr(VI) sorption. However, it could only perform well when no other competitive ions were present in the solution, severely impacting its application in complex, real matrices.

Keywords: Adsorption capacity; cation exchange; Cr isotopes; Cr(VI) reduction; Fe-modified zeolite; hexavalent chromium

(Received 7 October 2025 UTC; revised 9 March 2026 UTC; accepted 13 May 2026 UTC; Accepted Manuscript published online: 8 June 2026 UTC; Editor: George Christidis)

The oxidation states of Cr commonly found in nature are the trivalent form Cr(III) and the hexavalent form Cr(VI) (Rai *et al.*, 1989; Richard & Bourg, 1991; Kotaś & Stasicka, 2000; Magar *et al.*, 2008). In its trivalent state, Cr mainly forms insoluble or sparingly soluble compounds such as chromium oxide (mineral eskolaite, Cr_2O_3) and chromium hydroxide (minerals grimaldite, guyanite and bracewellite, $Cr(OH)_3$). The most common Cr(III) natural mineral is chromite ($(Mg,Fe^{2+})(Cr,Al,Fe^{3+})_2O_4$), belonging to the oxyspinel group, which is the main ore source for Cr. The solubility of Cr(III) increases in the presence of organic ligands (Hao *et al.*, 2022). In contrast, hexavalent chromium forms the chromate ion (CrO_4^{2-}) and the dichromate ion ($Cr_2O_7^{2-}$), both of which are highly soluble at the most common pH conditions of natural waters (Salem *et al.*, 1989; Unceta *et al.*, 2010). Figure 1 shows the Pourbaix diagram of chromium species in water under various pH and redox conditions.

Cr(III) is considered an essential micronutrient for the proper functioning of living organisms, while Cr(VI) exerts toxic effects on biological systems (Hossini *et al.*, 2022). This divergence in toxicological properties is intrinsically linked to the different chemical features exhibited by the two oxidation states (Tumolo *et al.*, 2020; Aharchaou *et al.*, 2022; Mortada *et al.*, 2023).

Compounds of Cr(VI) are mobile and bioavailable compared to the trivalent Cr species (Mandiwana *et al.*, 2007; Martello *et al.*, 2007). Due to its toxicity, chromium release into aquatic ecosystems is subject to regulation through international, national and local laws. In the European Union (EU) regulations, Cr is on the list of significant pollutants (Annex VIII – Water Framework Directive). Various international bodies within the EU, such as the Helsinki Commission (HELCOM) and the Oslo–Paris Convention (OSPAR), have issued recommendations regarding permissible emission levels of chromium compounds, most of which have been adopted and enforced by Member States. To maintain Cr(VI) in discharge waters below the legislated level, many industries are required to treat their effluents (Vaiopoulou & Gikas, 2020). A number of techniques have been used to remove hexavalent

Corresponding author: Bruno Freitas Pio de Azevedo;
Email: bruno.piodeazevedo@phd.unipi.it

Paper submitted for the special issue devoted to the ICC-2025

Cite this article: de Azevedo BFP, Panattoni F, Tardani M, Perchiazzi N, Ghezzi L and Mugnaioli E (2026) Comparative performance of iron-modified natural zeolites for chromium(VI) removal from aqueous solutions. *Clay Minerals* **61**, 239–255. https://doi.org/10.1180/clm.2026.10041

© The Author(s), 2026. Published by Cambridge University Press on behalf of The Mineralogical Society of the United Kingdom and Ireland.

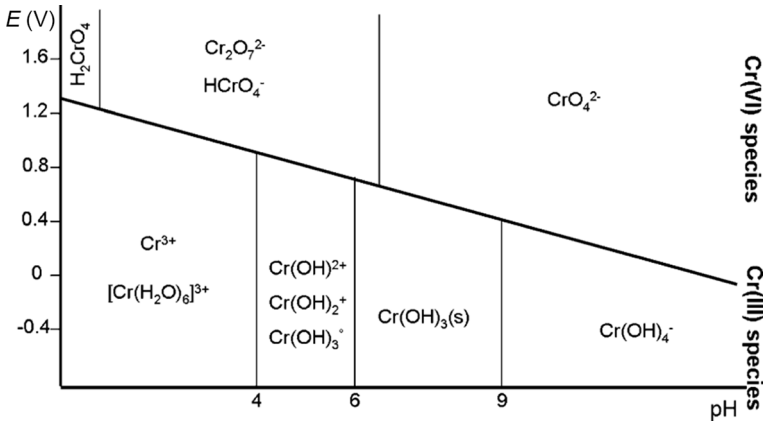


Figure 1. Pourbaix diagram showing the predominant chemical species of chromium in aqueous systems (after Unceta *et al.*, 2010). E = voltage potential.

chromium, but many of them have failed to bring contaminants down to an acceptable level according to the recommendations and guidelines of various agencies (Irshad *et al.*, 2023).

The typical method for eliminating Cr(VI) from industrial wastewater involves precipitation of Cr(III) hydroxide through redox reactions, facilitated by reducing agents such as sodium metabisulfite. However, this approach requires the use of substantial amounts of reagents, including sodium hydroxide, often resulting in elevated costs (Rosa *et al.*, 2021). Alternative methods for Cr(VI) removal include techniques such as membrane filtration, ion exchange, coagulation, reverse osmosis and chemical precipitation (Irshad *et al.*, 2023).

Among these, adsorption by zeolites appears particularly promising for eliminating pollutants from aqueous solutions. Zeolites are characterized by a three-dimensional porous structure with a high specific surface area and a large cation-exchange capacity (CEC). These characteristics give zeolites various advantageous physical and chemical properties, making them suitable for a wide range of water treatment applications, such as detergents, the removal of industrial pollutants, the removal of radionuclides from nuclear waste effluents, the treatment of acidic mine drainage waters and the recovery of heavy metals (Munthali *et al.*, 2014). To expand their applicability, zeolites may undergo various surface modifications or chemical alterations to make them compatible with various chemical species, such as oxyanions (Franus *et al.*, 2015; Suhartana *et al.*, 2018; Sumari *et al.*, 2018). In particular, zeolites modified with iron oxides/hydroxides and iron ions are valuable substrates for removing metals and metalloids in anionic form, such as Cr(VI) (Tashauoei *et al.*, 2010; Lv *et al.*, 2014; Chmielewská *et al.*, 2017).

There are several methods for modifying zeolites with iron, which can be divided into two main categories. The first category involves enriching the zeolite with Fe(II) ions, which act as reducing agents, promoting the reduction of Cr(VI) to Cr(III) within the zeolite structure (Døssing *et al.*, 2011; Bols *et al.*, 2021; Rosa *et al.*, 2022). The reduction of Cr(VI) to Cr(III) is a process that naturally occurs in the environment due to the presence of a number of electron donors, including Fe(II)-bearing phases (Brigatti *et al.*, 2000; Kiser & Manning, 2009). However, the kinetics of this reaction are generally very low, and it is common to use reducing agents such as catalysts to speed up this process (Kwak *et al.*, 2018). This category of zeolites is referred to as bivalent iron zeolites (BIZs).

The second category of modifications relies on the complexation of hexavalent chromium onto trivalent iron oxides/hydroxides at the surface of the zeolite (trivalent iron zeolite (TIZ)). Chromates, particularly at a low pH, tend to bond to the surfaces of hydrous ferric oxides (Villalobos *et al.*, 2001; Tzou *et al.*, 2003; Ajouyed *et al.*, 2010; Du *et al.*, 2012).

Both BIZ and TIZ show promise as viable alternatives for treating water contaminated with hexavalent chromium. However, a detailed comparative analysis to determine their relative effectiveness in Cr(VI) removal is currently lacking. Direct comparison of the adsorption capacity values reported in various studies is inherently challenging due to variations in analytical methodologies and experimental design. Differences in the type of natural zeolite (NZ) used, the modification technique, initial contaminant concentration, contact time, particle size, solid-to-liquid ratio, pH, ionic strength and temperature can significantly influence the calculated adsorption capacity. For example, Lofù *et al.* (2016) reported an adsorption capacity of 0.09 mg g^{-1} for an Fe(II)-modified NZ, whereas Rosa *et al.* (2021) measured a value of 0.9 mg g^{-1} under different experimental conditions, representing a 10-fold difference. Such discrepancies highlight how strongly adsorption capacity depends on the specific experimental framework rather than solely on the intrinsic properties of the modified material. Similar variability has also been reported for Fe(III)-modified zeolites.

For this reason, to provide a meaningful and scientifically sound comparison of material performance, it is essential to evaluate different modification strategies under identical experimental conditions, using the same original material. Only by controlling these variables can differences in removal efficiency be attributed to the modification approach itself rather than to circumstantial factors. Accordingly, this study presents a detailed physical and chemical characterization of BIZ and TIZ, together with a systematic evaluation of their efficacy in treating Cr(VI)-contaminated water, using both a synthetic solution and water collected from an actual polluted site.

Materials and methods

Chemicals and sorbent material

The NZ was purchased from Zeocel Italia. This material originates from Slovenia and consists of natural clinoptilolite zeolite grains with particle sizes 0.7–1.2 mm, with a specific surface area of 30m^2 g^{-1} and a CEC of 1.5–2.1 mol kg^{-1}. Other minor constituents are cristobalite, mica clay minerals, plagioclase and rutile according to the supplier's datasheet.

All of the reagents necessary for the synthesis of BIZ and TIZ and for the sorption experiments – ferrous sulfate heptahydrate ($FeSO_4{\cdot}7H_2O$), ferric chloride ($FeCl_3$), sodium hydroxide

https://doi.org/10.1180/clm.2026.10041 Published online by Cambridge University Press

(NaOH) and potassium dichromate ($K_2Cr_20_7$) – were purchased from Brenntag S.p.A.

Modified zeolites

The method proposed by Liu *et al.* (2010) and followed by Rosa *et al.* (2021) was applied to saturate the NZ with Fe(II) ions on its exchange sites. A total of 100 g of NZ was mixed with 1 L of a solution of 1 M $FeSO_4{\cdot}7H_2O$ at 50°C for 24 h to achieve the best conditions for modifying the zeolite with Fe(II). The mixture was then filtered and washed with distilled water, dried at 80°C overnight and stored in a desiccator. This modified zeolite is referred to as BIZ (bivalent iron zeolite).

A proprietary method developed by DND Biotech was used to precipitate trivalent iron oxides onto the surface of the NZ. In this process, the zeolite was immersed in a highly concentrated Fe(III) solution prepared from $FeCl_3$ and NaOH. The resulting modified material is referred to as TIZ (trivalent iron zeolite).

Synthetic solution and Cr(VI)-contaminated natural water

Various laboratory-produced synthetic solutions with varying Cr(VI) concentrations were prepared using demineralized water and $K_2Cr_2O_7$. One solution containing 29.2 mg L^{-1} of Cr(VI) was initially applied in the batch tests. Another solution, prepared with a lower concentration of 2.26 mg L^{-1} Cr(VI) to better approximate the concentration in real contaminated water, was used in both batch and column tests.

Additional solutions were prepared to evaluate the influence of pH and electrical conductivity (EC). The pH was adjusted using NaOH and nitric acid (HNO_3). To vary EC, pure demineralized water, pure tap water and four intermediate mixtures of the two at different proportions were employed. The tap water is characterized by a Ca–HCO_3 species, with the following major ion concentrations (mg L^{-1}): $Ca^{2+} = 58.9$; $Mg^{2+} = 14.7$; $Na^{+} = 41.1$; $K^{+} = 1.5$; $Cl^{-} = 41.5$; $SO_4{}^{2-} = 60.0$; and $HCO_3{}^{-} = 232.0$.

The real Cr(VI)-contaminated water was collected from a surface water body in an urban area severely contaminated by hexavalent chromium, released from pyrolysed tannery sludge wastes in central Italy (Ghezzi *et al.*, 2024). This water is characterized by a high salinity (EC of 1.2 mS cm^{-1}), pH 7.7 and a Cr(VI) concentration of 2.14 mg L^{-1}.

Batch tests and column tests

Batch tests were conducted to estimate the zeolite sorption capacity (Q) and to investigate the kinetics of Cr(VI) removal. Prior to the tests, the zeolites were washed with distilled water and dried at 80°C for at least 4 h. Batch and column tests were performed using both the Cr(VI)-bearing synthetic solution and the Cr(VI)-contaminated natural water.

To evaluate the effect of contact time on Cr(VI) removal, kinetic batch tests were performed using the synthetic solution with an initial Cr(VI) concentration of 29.2 mg L^{-1} (pH 7.6). For each run, 1 g of zeolite (NZ, BIZ or TIZ) was added to 100 mL of solution in polyethylene bottles and agitated at 120 rpm at room temperature. Aliquots were collected at t = 1, 3, 5, 7, 9, 24, 48, 72, 96 and 168 h. For dosage-dependent batch tests, Cr(VI) concentrations were determined after 24 and 168 h, selected on the basis of the kinetic test. In synthetic solution batch tests, variable amounts of zeolite (0.5, 1.0, 1.5, 2.0, 2.5 and 3.0 g) were added to 100 mL of the Cr(VI)-bearing solution; for natural contaminated water, 0.1, 0.2, 0.3, 0.4 and 0.5 g of zeolite were added to 100 mL of water. All tests were performed under agitation using an orbital shaker at 120 rpm at room temperature.

Additional batch tests with synthetic solutions were performed to evaluate the effect of pH on Cr(VI) removal. In these tests, 1.0 g of zeolite was added to Cr(VI)-containing solutions with pH values adjusted between 2.5 and 9.0. A similar procedure was applied to investigate the effect of EC, which was varied from 40 µS cm^{-1} (pure demineralized water with added Cr(VI)) to 600 µS cm^{-1} (tap water with added Cr(VI)). The determination of the final concentration of hexavalent chromium was carried out using a visible spectrophotometer (Iris HI801).

Synthetic solution column tests and natural Cr(VI)-contaminated water column tests were conducted using columns with an inner diameter of 10 mm and a height of 25 cm, filled with 1.0 g of modified zeolite. The system operated with a peristaltic pump, which pumped 0.3 L h^{-1} of the solution in a closed-cycle system.

The total Cr(VI) sorption (A, mg), the percentage of Cr(VI) removal (R, %) and the sorption capacity (Q, mg g^{-1}) were calculated according to Equations 1–3, respectively:

$$A = (C_i - C_t) \times V \tag{1}$$

$$R = (C_i - C_t)/C_i \times 100 \tag{2}$$

$$Q = A/W_Z \tag{3}$$

where C_i and C_t are the initial concentration and concentration of Cr(VI) (mg L^{-1}) at time t, respectively, V is the volume (L) of Cr(VI) solution and W_Z (g) is the weight of zeolite.

Adsorption isotherms

Adsorption isotherms (Langmuir and Freundlich models) were applied to the dataset of the batch tests, consisting of data from 168 h of contact between the synthetic solution and the zeolites. The Langmuir isotherm is described by Equation 4:

$$Q = \frac{Q_{max} \times K_L \times C_t}{1 + K_L \times C_t} \tag{4}$$

where Q_{max} represents the maximum adsorption capacity (mg g^{-1}) and K_L is the Langmuir isotherm constant, which shows the binding affinity between the adsorbent and the adsorbate. The Freundlich isotherm is given by Equation 5:

$$Q = K_F \times C_t^{1/n} \tag{5}$$

where K_F is the Freundlich constant used to measure the adsorption capacity and $1/n$ is the adsorption intensity. The value of $1/n$ defines whether the adsorption process is either favourable ($0.1 < 1/n < 0.5$) or unfavourable ($1/n > 2$).

Cr isotope analysis

The $^{53}Cr/^{52}Cr$ ratio of Cr(VI) in water from batch experiments was measured by multicollector inductively coupled plasma mass spectrometry (MC-ICP-MS; AlS Scandinavia AB; Neptune PLUS, Thermo Scientific, Bremen, Germany) using a combination of internal standardization and external calibration (Pontér *et al.*, 2016). The measured $^{53}Cr/^{52}Cr$ ratios were expressed using the

https://doi.org/10.1180/clm.2026.10041 Published online by Cambridge University Press

Table 1. Evolution of residual Cr(VI) concentration (mg L^{-1}) over time in the batch tests.

Zeolite	0 h	1 h	3 h	5 h	7 h	9 h	24 h	48 h	72 h	96 h	168 h
NZ	29.2	29.0	29.1	28.8	28.9	28.8	29.0	28.9	28.7	28.9	28.8
BIZ	29.2	28.7	28.1	27.3	26.6	25.9	21.3	18.6	16.7	15.3	14.4
TIZ	29.2	25.6	23.1	21.2	20.5	19.9	18.4	17.4	17.2	17.3	17.2

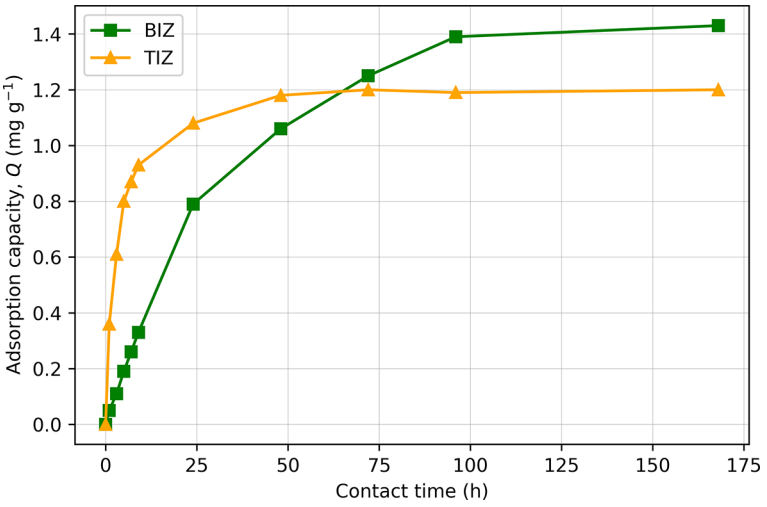


Figure 2. Effect of contact time on adsorption capacity (Q) for BIZ and TIZ in the batch experiments. TIZ exhibits rapid Cr(VI) uptake and early saturation, whereas BIZ shows a slower but continuous increase in adsorption capacity.

conventional δ notation referred to the NIST SRM 979 standard and as shown in Equation 6:

$$\delta^{53}\mathrm{Cr} = \left(\left({}^{53}\mathrm{Cr}/{}^{52}\mathrm{Cr}_{\mathrm{sample}}/{}^{53}\mathrm{Cr}/{}^{52}\mathrm{Cr}_{\mathrm{SRM\ 979}}\right) - 1\right) \times 1000 \quad (6)$$

The acceptance criterion is that δ^{53}Cr for purified Cr does not differ from the value before purification by more than 1‰. Recovery after column chemistry should be better than 90%. The chromium isotope fractionation between the various Cr species allows detection of Cr reduction in aqueous environments (Li *et al.*, 2022). The amount of Cr(VI) reduction to Cr(III) can be traced isotopically, as the δ^{53}Cr value of the residual Cr(VI) in solution progressively increases following a Rayleigh-type function (Ellis *et al.*, 2002; Kitchen *et al.*, 2012).

Zeolite characterization

NZ, BIZ and TIZ were characterized by X-ray powder diffraction (XRPD), X-ray fluorescence (XRF) spectroscopy, scanning electron microscopy (SEM) and transmission electron microscopy (TEM) at the Dipartimento di Scienze della Terra of the Università di Pisa and at the Center for Instrument Sharing of the University of Pisa (CISUP). The BIZ and TIZ samples were analysed before and after sorption experiments in batches.

The XRPD data were collected on a Bruker D2 phaser diffractometer, equipped with a Lynxeye detector, operating at 30 kV and 10 mA and using Cu-$K\alpha$ radiation ($\lambda = 1.54184$ Å). Identification of the crystalline phases was carried out with *EVA-Bruker* software (Bruker AXS, Karlsruhe, Germany), using the PDF2-2023 database (Gates-Rector & Blanton, 2019), and these results were further validated through Rietveld refinement of the XRPD traces (Bish & Post, 1993; Young, 1993), carried out with *Topas-Academic* v7 software (Coelho, 2018). XRF analysis was performed with a Niton™ XL3t XRF analyser on a few grams of loose and dried grains from the various zeolite samples.

A Hitachi tabletop 3030plus SEM device was used to visualize the external surfaces of loose zeolite grains and the internal cross-sections of grains embedded in resin and milled along a planar surface. An integrated energy-dispersive X-ray spectroscopy (EDS) device was used for elemental analysis and mapping to identify zones of interest for further detailed analysis. TEM analysis was performed using a JEOL JEM-F200 device working at 200 kV and equipped with a Schottky field emission gun source. TEM images were acquired with a Gatan RIO16 CMOS camera (4k × 4k). EDS point analysis and elemental mapping were performed with a JEOL SSD detector.

Nitrogen adsorption–desorption isotherms were obtained with a Gemini 2375 Series surface area analyser (Micromeritics). Samples were degassed for 4 h at 160°C under a continuous flow of nitrogen gas prior to analysis. The calculation of the specific surface area was carried out using the Brunauer–Emmett–Teller (BET) method. These measurements were conducted at the Dipartimento di Ingegneria Civile e Meccanica, Università degli Studi di Cassino e del Lazio Meridionale.

Results and discussion

Effect of contact time on Cr(VI) removal in synthetic batch tests

The temporal evolution of residual Cr(VI) concentrations in the presence of NZ, BIZ and TIZ is listed in Table 1. The synthetic solution had an initial Cr(VI) concentration of 29.2 mg L^{-1}, a pH of 7.6 and an EC of 60 µS cm^{-1}. NZ did not adsorb Cr(VI) throughout the experiment. This confirms that unmodified clinoptilolite has no significant affinity for chromate under the investigated conditions.

In contrast, both modified zeolites exhibited a progressive decrease in Cr(VI) concentration, although with markedly different kinetic behaviours. Figure 2 illustrates this difference by showing the evolution of adsorption capacity (Q) as a function of contact time.

https://doi.org/10.1180/clm.2026.10041 Published online by Cambridge University Press

Table 2. Batch test results for the 24 h experiment with synthetic solution.

	BIZ				TIZ			
Zeolite (g)	C_t (mg L^{-1})	A (mg)	R (%)	Q (mg g^{-1})	C_t (mg L^{-1})	A (mg)	R (%)	Q (mg g^{-1})
0.5	25.1	0.41	14.04	0.82	24.35	0.48	16.61	0.97
1.0	21.8	0.77	26.37	0.77	18.20	1.10	37.67	1.10
1.5	20.9	0.83	28.42	0.55	13.70	1.54	52.91	1.03
2.0	18.3	1.11	38.01	0.56	13.34	1.57	53.94	0.79
2.5	17.4	1.18	40.41	0.47	10.20	1.90	65.07	0.76
3.0	15.7	1.35	46.23	0.45	8.90	2.03	69.52	0.68

A = total Cr(VI) sorption; C_t = Cr(VI) concentration at 24 h; Q = sorption capacity; R = removal rate.

Table 3. Batch test results for the 168 h experiment with synthetic solution.

	BIZ				TIZ			
Zeolite (g)	C_t (mg L^{-1})	A (mg)	R (%)	Q (mg g^{-1})	C_t (mg L^{-1})	A (mg)	R (%)	Q (mg g^{-1})
0.5	20.1	0.91	31.16	1.82	23.30	0.59	20.21	1.18
1.0	14.4	1.48	50.58	1.48	17.20	1.20	41.10	1.20
1.5	10.1	1.91	65.41	1.27	12.35	1.68	57.71	1.12
2.0	7.6	2.16	73.97	1.08	9.40	1.98	67.81	0.99
2.5	4.85	2.43	83.39	0.97	6.30	2.29	78.42	0.92
3.0	3.25	2.59	88.87	0.86	4.70	2.45	83.90	0.82

A = total Cr(VI) sorption; C_t = Cr(VI) concentration at 168 h; Q = sorption capacity; R = removal rate.

Table 4. Isotopic analysis from BIZ and TIZ after 168 h synthetic solution batch tests.

Sample	C_t (mg L^{-1})	δ^{53}Cr (‰)	2 SD (‰)
BIZ 1 g	14.4	1.790	0.064
BIZ 2 g	7.60	2.354	0.056
BIZ 3 g	3.25	3.834	0.093
TIZ 1 g	17.2	0.345	0.064
TIZ 2 g	9.40	0.334	0.076
TIZ 3 g	4.70	0.314	0.062

2 SD = standard deviation; δ^{53}Cr = conventional δ-notation for the ^{53}Cr/^{52}Cr ratio of Cr(VI); C_t = Cr(VI) concentration at 168 h.

BIZ displays a slower but continuous increase in adsorption capacity over the entire experimental duration, reaching a higher Q value (~1.43 mg g^{-1}) after 168 h. No further Cr(VI) removal was detected beyond this time, suggesting that equilibrium was eventually reached. This kinetic behaviour is consistent with the proposed removal mechanism. Extra-framework Fe^{2+} ions are progressively released into solution according to ion-exchange equilibrium. Once in solution, Fe^{2+} acts as a reducing agent, converting Cr(VI) to Cr(III) in a subsequent redox reaction. Once Fe^{2+} is consumed during reduction, the exchange equilibrium shifts to release additional Fe^{2+} from the zeolite matrix, and the process continues until the available pool of exchangeable Fe^{2+} is depleted.

In contrast, TIZ shows a rapid increase in adsorption capacity during the first hours, reaching near-equilibrium conditions between 24 and 48 h, with a maximum Q of 1.2 mg g^{-1}. This behaviour is consistent with a fast, adsorption-controlled mechanism on Fe(III)-(oxy)hydroxide surface sites, as reported in kinetic studies describing Cr(VI) uptake by Fe(III) phases, which commonly follow pseudo-second-order adsorption kinetics (Yu & Zhang, 2014; Sultana *et al.*, 2021).

Based on these kinetic trends, 24 h was selected as a representative short contact time, sufficient for TIZ to approach its near-saturation point (~90% of its adsorption capacity), and consistent with contact times commonly adopted in many others batch adsorption studies, whereas 168 h was used to approximate equilibrium conditions for BIZ in batch experiments.

As stated previously, direct comparison of adsorption capacity values (Q) reported in the literature is not straightforward due to significant differences in experimental conditions. Rosa *et al.* (2022) investigated an Fe(II)-modified zeolite and reported a Q value of ~0.9 mg g^{-1}, which is in agreement with the present results when considering that their experiments were conducted at a lower initial Cr(VI) concentration (18.5 mg L^{-1}) and with a contact time of 24 h. Rosa *et al.* (2022) reported the removal of nearly 100% of the available Cr(VI) from solution, suggesting that the actual adsorption capacity of the material may be higher than the reported value.

To the best of our knowledge, no comparable studies are available in the literature reporting batch adsorption experiments using Fe(III)-modified zeolites with synthetic solutions containing only Cr(VI), which limits the possibility of making direct comparisons.

Effect of zeolite dosage on Cr(VI) removal in synthetic batch tests

Batch experiments with increasing zeolite dosages were analysed to evaluate the influence of the amount of sorbent on Cr(VI) removal efficiency and adsorption capacity. The initial Cr(VI) concentration in the synthetic solution was 29.2 mg L^{-1} at pH 5.6. Increasing amounts of BIZ and TIZ (0.5–3.0 g 100 mL^{-1}) were tested. NZ was also included, but, once again, regardless of the quantity of zeolite used, the final concentrations were comparable to the initial concentration. The results of the batch tests for BIZ and TIZ with synthetic solution after 24 and 168 h are listed in Tables 2 & 3, respectively.

As expected, after 24 h TIZ exhibits a better efficiency for removing Cr(VI) from the synthetic solution compared to BIZ, with the difference increasing as dosage increases. With 0.5 g

https://doi.org/10.1180/clm.2026.10041 Published online by Cambridge University Press

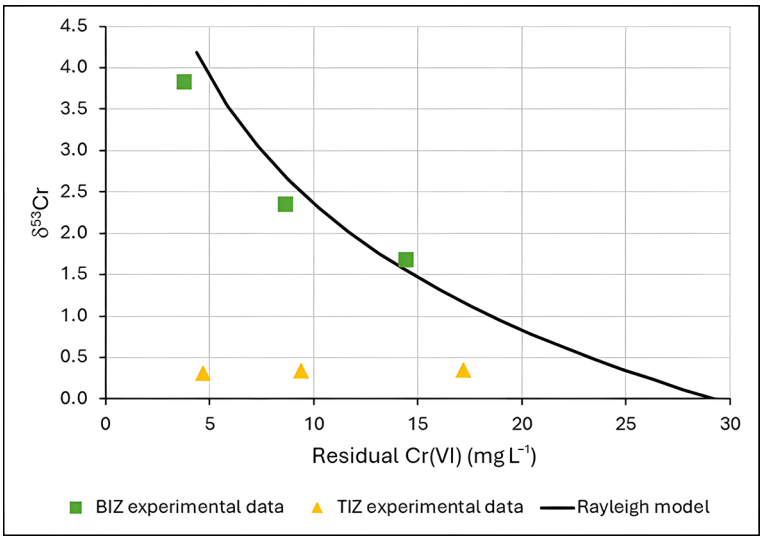


Figure 3. Rayleigh isotopic fractionation model and $\delta^{53}Cr$ experimental data for BIZ and TIZ.

of zeolite, the removal efficiencies are 16.61% for TIZ and 14.04% for BIZ. When the zeolite dosage increases to 3.0 g, the removal efficiencies increase to 69.52% for TIZ and 46.23% for BIZ.

The trends of chromium removal are reversed by the end of the experiment at 168 h, when saturation is reached, with BIZ showing better performance in terms of Cr(VI) removal from the synthetic solution, as 0.5 g BIZ removed 31.16% of Cr(VI), with a Q value of 1.81, while the same amount of TIZ removed 20.21% of Cr(VI), with a Q value of 1.18. Both zeolites show similar trends until reaching the highest Cr(VI) removal percentages of 88.87% and 83.90% when using 3.0 g of BIZ and TIZ, respectively.

Isotopic analysis

To $\delta^{53}Cr$ values determined on some synthetic solutions used for the batch experiments are listed in Table 4.

In general, Cr(VI) from both geogenic and anthropogenic sources is characterized by a $\delta^{53}Cr$ of ~0. Positive $\delta^{53}Cr$ values are generally interpreted as a reduction of Cr(VI) to Cr(III). In the TIZ experiments the $\delta^{53}Cr$ remains quite constant, indicating that no significant Cr(VI) reduction occurred. In contrast, the positive $\delta^{53}Cr$ values obtained for the BIZ experiments provide evidence of Cr(VI) reduction. Furthermore, the correspondence of the experimental $\delta^{53}Cr$ data and C_t is well fitted by a Rayleigh equation model (Fig. 3), indicating a fractionation factor (α) of 0.9978. This value is consistent with the isotopic fractionation expected for abiotic Cr(VI) reduction by Fe(II) (Kitchen *et al.*, 2012; Li *et al.*, 2022).

Thus, BIZ acts as a reactive medium for chromium reduction, with Fe(II) serving as the primary reducing agent. Similar conclusions have been proposed by Lv *et al.* (2014), who related the extent of Cr(VI) removal to the amount of Fe(II) exchanged onto the zeolite grains. However, those interpretations were based on indirect correlations. In contrast, the present study provides direct evidence of the reduction mechanism through chromium isotope analysis, which confirms that Cr(VI) removal by BIZ involves a redox transformation.

Adsorption isotherms

Experimental data from synthetic solution batch tests with TIZ are better modelled by a Freundlich isotherm, with a coefficient of determination (R^2) of 0.98, while with a Langmuir isotherm R^2 is only 0.82 (Fig. 4). Therefore, TIZ probably behaves as a multilayer adsorbent of Cr(VI), and the sorption is probably heterogeneous on its surface. The Freundlich isotherm parameters obtained by fitting are $K_F = 0.61$ and $1/n = 0.22$.

These results are in accord with Du *et al.* (2012), who also reported that the Freundlich model provided a better description of the adsorption behaviour than the Langmuir model, obtaining R^2 values of 0.94 and 0.71, respectively.

Batch test with real contaminated water

The results of the batch test for the real water sample from a contaminated site are reported in Table 5. The Cr(VI) removal efficiency for TIZ is dramatically lower compared to the results from the synthetic solution batch experiments. Conversely, BIZs achieve a Cr(VI) removal efficiency of ~98.1% at 0.5 g, which is higher than any value obtained in the batch experiments.

The difference in the efficiency of TIZ could be related to the main mechanism involved in this process. TIZ acts as a direct adsorption substrate that, in the presence of competing ions for the adsorption sites, does not perform as expected due to a stronger affinity for other anions. Suhartana *et al.* (2018) have demonstrated that Fe(III)-modified zeolite also directly adsorbs chloride and carbonate ions onto its surface. In addition, the main mechanism of BIZ is the reduction of Cr(VI) to Cr(III) catalysed by Fe(II) ions, which appears not to be affected by the presence of other ions in the solution.

The adsorption capacity values for TIZ obtained in this experiment are comparable to those reported by Du *et al.* (2012) for Fe(III)-modified zeolite, who observed Q values ranging from 0.01 to 0.06 mg g^{-1} under high-ionic-strength conditions.

https://doi.org/10.1180/clm.2026.10041 Published online by Cambridge University Press

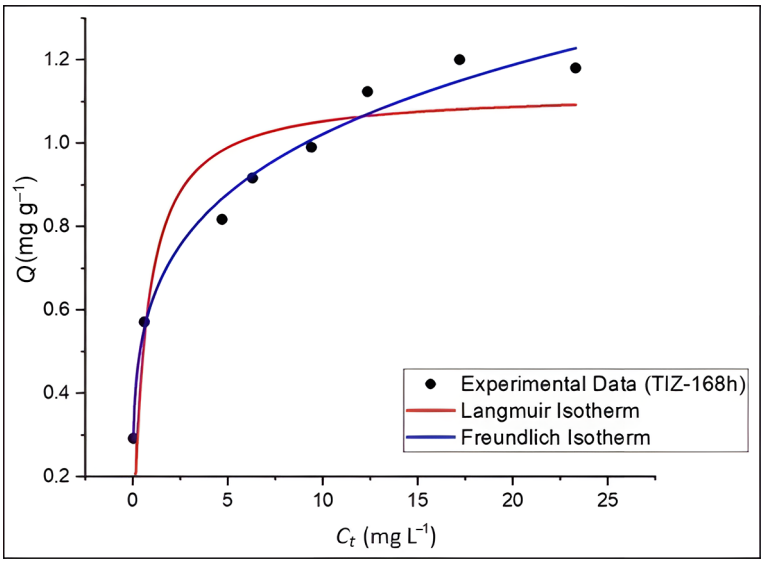


Figure 4. Experimental data from TIZ and Langmuir and Freundlich isotherm models.

Table 5. Batch test results for the 168 h experiments with real water.

	BIZ				TIZ			
Zeolite (g)	C_t (mg L^{-1})	A (mg)	R (%)	Q (mg g^{-1})	C_t (mg L^{-1})	A (mg)	R (%)	Q (mg g^{-1})
0.1	1.46	0.07	31.78	0.68	2.06	0.01	3.74	0.08
0.2	0.76	0.14	64.49	0.69	2.05	0.01	4.21	0.05
0.3	0.47	0.17	78.04	0.56	2.01	0.01	6.07	0.04
0.4	0.14	0.20	93.46	0.50	1.98	0.02	7.48	0.04
0.5	0.04	0.21	98.13	0.42	1.92	0.02	10.28	0.04

A = total Cr(VI) sorption; C_t = Cr(VI) concentration at 168 h; Q = sorption capacity; R = removal rate.

Table 6. Batch test results from the synthetic solution with varying pH values.

	BIZ				TIZ			
pH	C_t (mg L^{-1})	A (mg)	R (%)	Q (mg g^{-1})	C_t (mg L^{-1})	A (mg)	R (%)	Q (mg g^{-1})
2.5	7.2	1.13	61.1	1.13	12.3	0.62	33.5	0.62
3.8	7.2	1.13	61.1	1.13	12.0	0.65	35.1	0.65
5.2	7.1	1.14	61.6	1.14	11.6	0.69	37.3	0.69
6.5	7.3	1.12	60.5	1.12	11.4	0.71	38.4	0.71
7.2	8.0	1.05	56.8	1.05	12.5	0.60	32.4	0.60
9.0	8.3	1.02	55.1	1.02	13.2	0.53	28.6	0.53

A = total Cr(VI) sorption; C_t = Cr(VI) concentration at 168 h; Q = sorption capacity; R = removal rate.

Influence of pH and EC

The effects of pH and EC in the batch experiments were examined with additional specific tests. A synthetic solution made with demineralized water and an initial Cr(VI) concentration of 18.5 mg L^{-1} was used, at pH 2.5–9.0. The results are reported in Table 6. BIZ shows more constant behaviour and consistently outperforms TIZ under all tested conditions. Both materials exhibit optimal removal under mildly acidic conditions (pH 5.0–6.5). TIZ shows a moderate decrease in efficiency under strongly acidic conditions and a pronounced decrease in efficiency under alkaline conditions, whereas BIZ is mainly affected only under alkaline conditions. These results demonstrate that pH has an effect on the efficiency of BIZ and TIZ for Cr(VI) removal but cannot explain the significant reduction in the performance of TIZ in the real-water batch test.

The batch test results from a 24 h experiment, carried out under different EC conditions (pH = 6.7; initial Cr(VI) concentration = 18.5 mg L^{-1}), are summarized in Table 7 and illustrated in Fig. 5. TIZ performs very well when Cr(VI) is the only anion present in the solution (pure demineralized water with added Cr(VI) reagent; EC = 40 μS cm^{-1}). However, when competing ions are present, its performance decreases rapidly. This indicates that TIZ has a stronger affinity for other major anions, which severely limits its effectiveness in complex water matrices.

However, BIZ exhibits the opposite trend, with its performance increasing as salinity increases. The main hypothesis to explain this behaviour is that a higher concentration of cations in solution improves the cation-exchange process. As more exchangeable cations become available, Fe^{2+} ions at extra-framework zeolite sites can be readily released, acting as reducing agents to convert Cr(VI) to Cr(III). In conditions with low cation availability, Fe^{2+}

https://doi.org/10.1180/clm.2026.10041 Published online by Cambridge University Press

Table 7. Batch test results from the synthetic solution with varying EC values.

	BIZ				TIZ			
EC (μS cm^{-1})	C_t (mg L^{-1})	A (mg)	R (%)	Q (mg g^{-1})	C_t (mg L^{-1})	A (mg)	R (%)	Q (mg g^{-1})
40	12.9	0.56	30.3	0.56	8.7	0.98	53.0	0.98
120	12.5	0.60	32.4	0.60	14.9	0.36	19.5	0.36
240	12.4	0.61	33.0	0.61	15.0	0.35	18.9	0.35
360	12.2	0.63	34.1	0.63	14.6	0.39	21.1	0.39
480	12.1	0.64	34.6	0.64	15.6	0.29	15.7	0.29
600	11.8	0.67	36.2	0.67	15.7	0.28	15.1	0.28

A = total Cr(VI) sorption; C_t = Cr(VI) concentration at 24 h; Q = sorption capacity; R = removal rate.

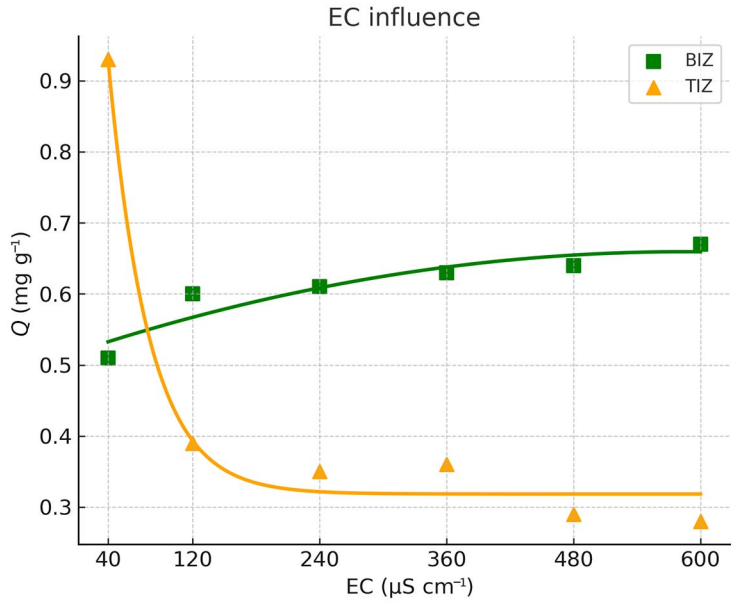


Figure 5. Adsorption capacity (Q) of BIZ and TIZ in batch tests as a function of EC.

ions are also required to balance the negative charge of the zeolite framework, limiting their availability for redox reactions.

These results are consistent with those of Lv *et al.* (2014), who studied Fe(II)-modified NZ and observed a ∼20% increase in Cr(VI) sorption as the ionic strength increased from 0.0001 mol L^{-1} of NaCl to 0.1 mol L^{-1} of NaCl in the contaminated solution.

Column tests

The column setup operated in a closed-loop configuration, meaning that the effluent from the column was recirculated back into the influent reservoir. At a flow rate of 0.3 L h^{-1}, the 1 L solution passed through the column containing 1 g of modified zeolite approximately seven times during the experiment.

The results of the column experiments for the synthetic solution with an initial concentration of Cr(VI) of 2.26 mg L^{-1} are reported in Table 8, while the results of the column experiments with real water with an initial concentration of Cr(VI) of 2.14 mg L^{-1} are listed in Table 9.

The column tests performed with a lower concentration of Cr(VI) using a synthetic solution, without other major anions, showed that TIZ has a higher adsorption capacity (Q = 1.09 mg g^{-1}) and a faster kinetic removal rate compared to BIZ (Q = 0.66 mg g^{-1}). However, in line with the batch tests, TIZ's performance changes dramatically when the column tests are performed with real water. When applied to a complex real water with high salinity, TIZ removes only 2.80% of the initial Cr(VI) content (Q = 0.06 mg g^{-1}), while BIZ is more efficient, achieving ∼34.11% Cr(VI) removal (Q = 0.73 mg g^{-1}). These results corroborate previous experiments, demonstrating that the adsorption capacity of BIZ is higher with real water than with the synthetic solution. Figure 6 demonstrates the removal rate from each experiment as a function of the treated volume.

XRPD analysis

The XRPD traces of NZ, BIZ and TIZ essentially overlap, indicating that the samples are made up of the same mineral phases with essentially the same abundances (Fig. 7). The predominant mineral phase is clinoptilolite/heulandite, constituting ∼75 wt.% of the bulk sample. Minor phases are albitic plagioclase (∼15 wt.%), orthoclase (5 wt.%), muscovite and quartz (5 wt.% total).

BET analysis and nitrogen adsorption–desorption isotherms

The results for specific surface area and porosity are summarized in Table 10. The observed difference in BET specific surface area is mainly attributed to variations in the micropore area, which are also reflected in differences in micropore volume, while the external surface area is similar for both materials. This difference is attributed to the precipitation of iron(III) phases and other

https://doi.org/10.1180/clm.2026.10041 Published online by Cambridge University Press

Table 8. TIZ and BIZ results from the column tests of the synthetic solution.

	BIZ				TIZ			
Time	C_t (mg L^{-1})	A (mg)	R (%)	Q (mg g^{-1})	C_t (mg L^{-1})	A (mg)	R (%)	Q (mg g^{-1})
3 h	1.92	0.34	15.04	0.34	1.72	0.54	23.89	0.54
6 h	1.83	0.43	19.03	0.43	1.52	0.74	32.74	0.74
9 h	1.71	0.55	24.34	0.55	1.28	0.98	43.36	0.98
12 h	1.65	0.61	26.99	0.61	1.19	1.07	47.35	1.07
24 h	1.60	0.66	29.20	0.66	1.17	1.09	48.23	1.09

A = total Cr(VI) sorption; C_t = Cr(VI) concentration at time t; Q = sorption capacity; R = removal rate.

Table 9. TIZ and BIZ results from the column tests of real water.

	BIZ				TIZ			
Time	C_t (mg L^{-1})	A (mg)	R (%)	Q (mg g^{-1})	C_t (mg L^{-1})	A (mg)	R (%)	Q (mg g^{-1})
3 h	1.99	0.15	7.01	0.15	2.12	0.02	0.93	0.02
6 h	1.85	0.29	13.55	0.29	2.1	0.04	1.87	0.04
9 h	1.67	0.47	21.96	0.47	2.08	0.06	2.80	0.06
12 h	1.51	0.63	29.44	0.63	2.09	0.05	2.34	0.05
24 h	1.41	0.73	34.11	0.73	2.08	0.06	2.80	0.06

A = total Cr(VI) sorption; C_t = Cr(VI) concentration at time t; Q = sorption capacity; R = removal rate.

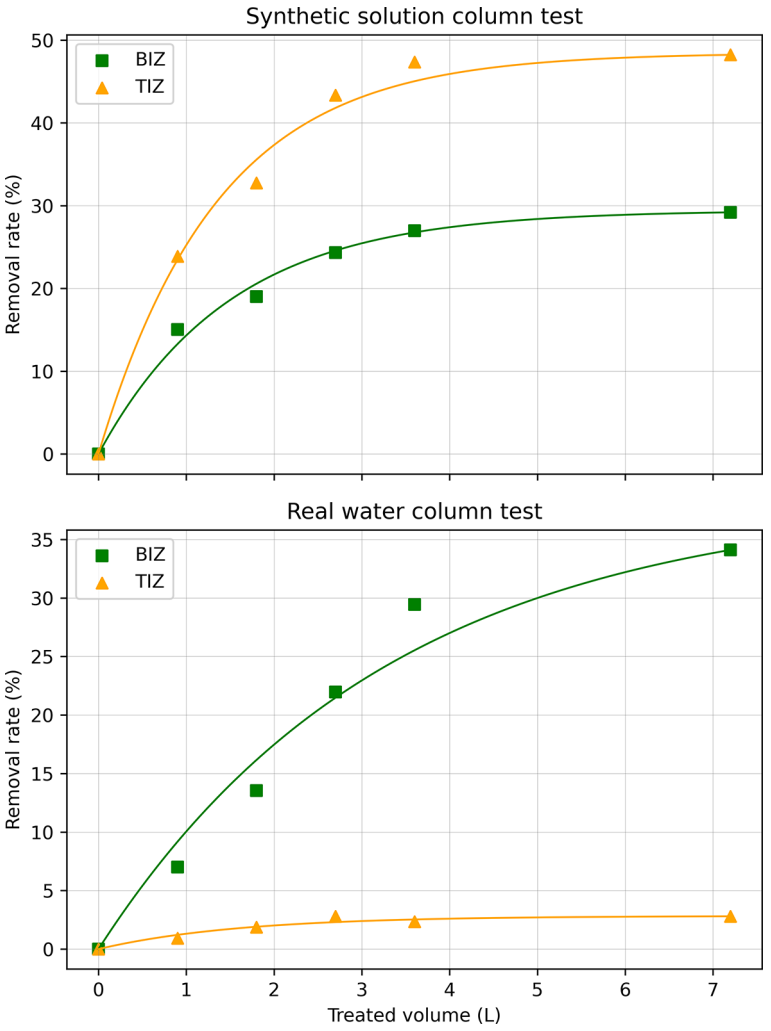


Figure 6. Removal efficiency (%) of Cr(VI) in bulk solution as a function of treated volume (L) during the column experiments. Top: synthetic Cr(VI) solution; bottom: real contaminated water.

https://doi.org/10.1180/clm.2026.10041 Published online by Cambridge University Press

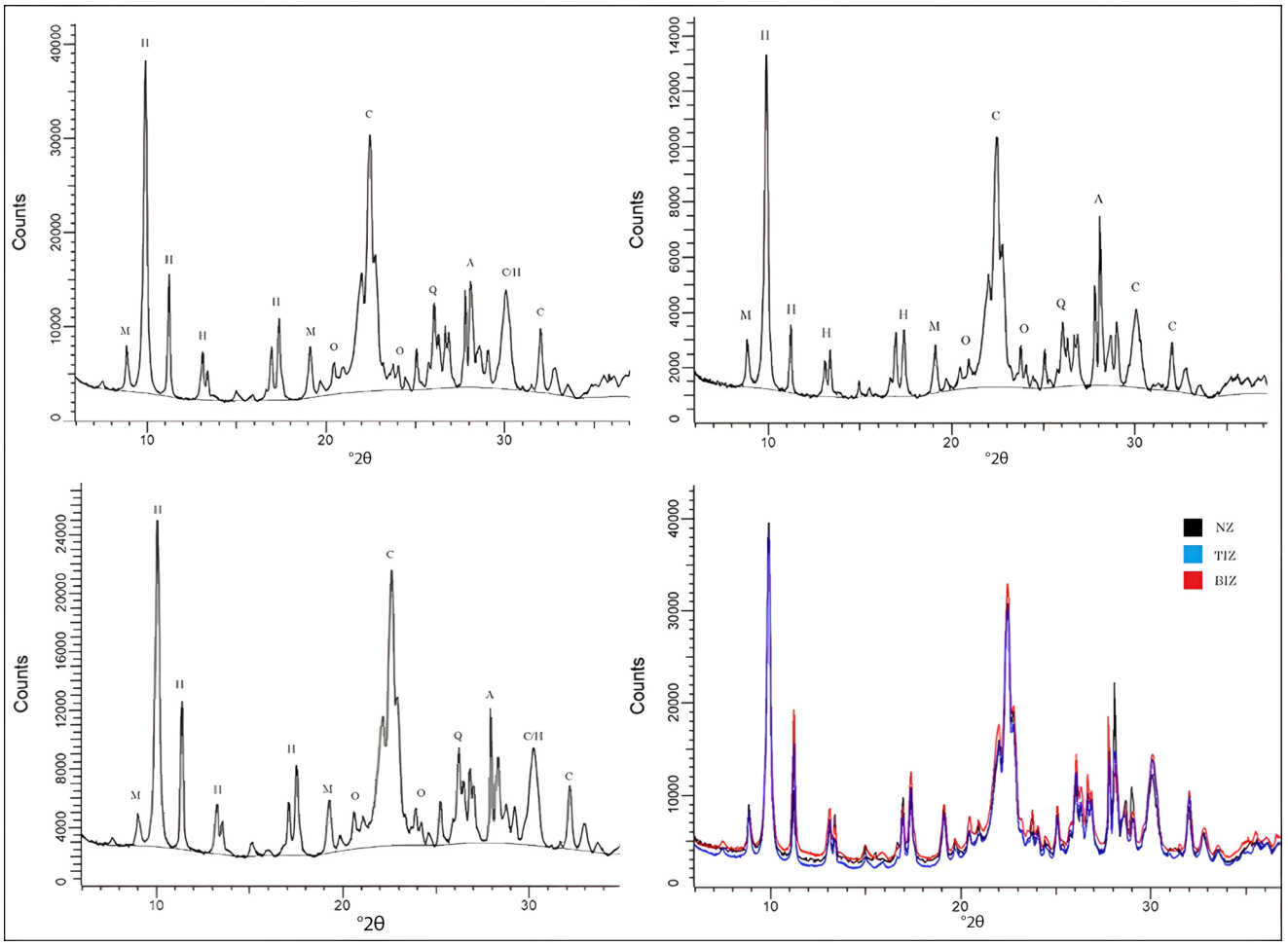


Figure 7. (Top left) XRPD trace from the NZ sample; (top right) XRPD trace from the BIZ sample; (bottom left) XRPD trace from the TIZ sample; (bottom right) XRPD traces from NZ, BIZ and TIZ superimposed and normalized. A = albitic plagioclase; C = clinoptilolite; H = heulandite; M = muscovite; O = orthoclase Q = quartz.

Table 10. Results from the BET analysis.

Sample	BET specific surface area ($m^2\ g^{-1}$)	External surface area ($m^2\ g^{-1}$)	Micropore area ($m^2\ g^{-1}$)	Micropore volume ($cm^3\ g^{-1}$)
BIZ	42.92	27.94	14.97	0.006356
TIZ	28.84	26.13	2.71	0.000917

salts during the TIZ modification process previously discussed. These precipitates are not only visible on the external surface but also appear to partially occupy mesopores, fractures and structural defects within the material, contributing to the reduction of micropore area and volume (see Supplementary Material).

Nitrogen adsorption–desorption isotherms are reported in Fig. 8. According to the Brunauer–Deming–Deming–Teller (BDDT) classification, both isotherms correspond to type IV behaviour, exhibiting a clear H4-type hysteresis loop in the desorption branch.

XRF spectroscopy

XRF spectroscopy confirms the results obtained by the adsorption experiments (Table 11). The iron weight percentage increased in both BIZ (5.18 wt.%) and TIZ (4.28 wt.%) compared to NZ (1.08 wt.%). In the case of BIZ, a significant increase in sulfur and a decrease in potassium support the occurrence of reagent impregnation and cation exchange, respectively. For TIZ, chloride is present in the initial product. However, most chlorine was probably dissolved during the batch test, as indicated by a substantial decrease in chorine following the batch experiment. Both BIZ and TIZ, when saturated with Cr, show up to a 10-fold increase in Cr content compared to their initial concentrations.

SEM macrostructural analysis and TEM microstructural analysis

Natural zeolite

The NZ grains exhibit a polyhedral morphology, deviating significantly from a spherical geometry. Each face is characterized by an undulated topology, marked by continuous micro-scale elevations and depressions (Fig. 9a). At a higher magnification, the grain surfaces are highly irregular, with a variety of micro-grains attached to a more coherent solid matrix (Fig. 9b).

Cross-section SEM images of grains embedded in resin reveal the internal structure of the material. Morphologically, the internal features broadly mirror the external surface, although with variable degrees of structural coherence. Certain domains appear relatively compact and homogeneous, while others display a granular

https://doi.org/10.1180/clm.2026.10041 Published online by Cambridge University Press

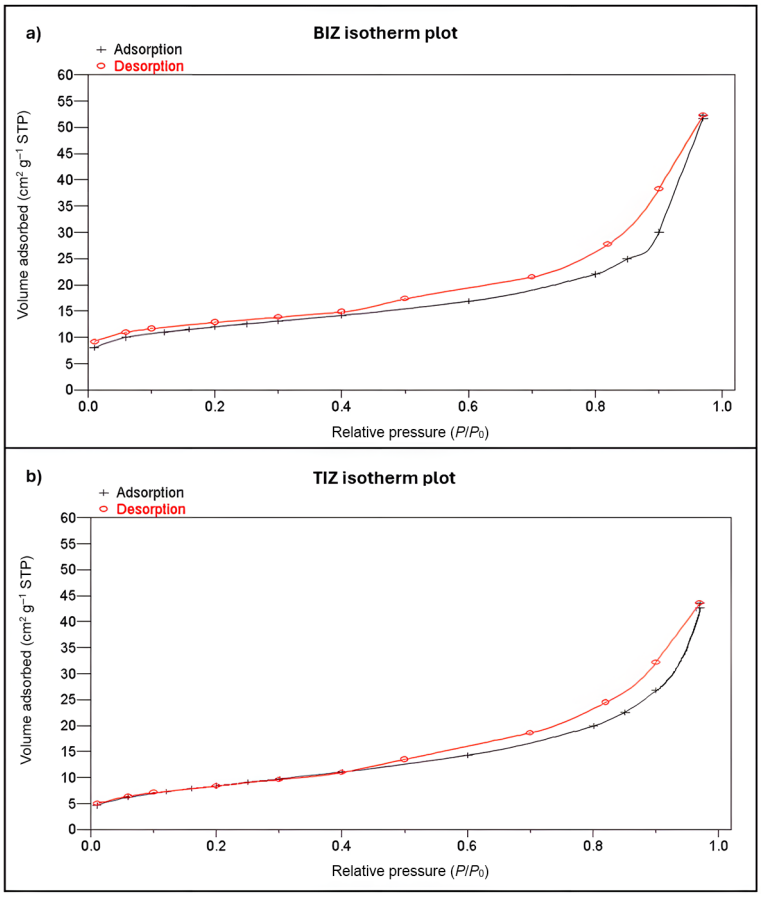


Figure 8. Nitrogen adsorption–desorption isotherms from (a) BIZ and (b) TIZ. STP = standard temperature and pressure.

Table 11. XRF spectroscopy results (wt.%) of the materials used in the experiments.

	Sample				
Element	NZ	BIZ	BIZ after batch test	TIZ	TIZ after batch test
Al	6.4680	6.1444	6.2805	6.1506	5.7841
Ca	2.1370	2.2297	2.4028	2.8793	2.8672
Cl	0.0529	0.0771	0.1962	4.2430	0.4143
Cr	0.0009	0.0026	0.0315	0.0025	0.0283
Fe	1.0840	5.1777	4.0912	4.2789	3.9455
K	2.2150	1.4817	1.8700	2.3272	2.7279
Mg	0.5768	1.6494	2.5593	1.9364	2.3978
S	0.4256	1.7610	2.0683	0.3951	0.5479
Si	29.3408	27.4204	26.4893	26.0101	27.5638

texture, with visible macroporosity. Both zeolite domains appear chemically homogeneous under EDS analysis, with a chemistry that is broadly consistent with typical clinoptilolite–heulandite. However, grains of other mineral phases are heterogeneously distributed within the clinoptilolite grain, and especially in granular domains (Fig. 10a). At higher magnifications, the host phases show a broad size distribution, often being below 1 μm in size (Fig. 10b). EDS analyses suggest that most of the largest secondary grains are plagioclase or orthoclase.

Bivalent iron zeolite

Morphologically, the BIZ grains do not differ significantly from their NZ counterparts (Fig. 11). However, their chemical composition shows notable differences. Iron and sulfur are present in high concentrations, indicating an excess of the modifying reagent $FeSO_4 \cdot 7H_2O$. The method proposed by Liu *et al.* (2010) was not intended to produce a coating on the zeolite surface; however, at the applied reagent concentrations, impregnation of the reagent occurs, forming a surface layer that imparts the green colouration observed.

Nevertheless, the objective of increasing the Fe^{2+} content through cation exchange appears to have been successfully achieved. Within the grains, EDS analysis revealed no significant sulfur signal, while the iron concentration increased markedly compared to the atomic percentage in NZ, increasing from an average of 1.0 wt.% to values higher than 3.0 wt.%. This increase was accompanied by a pronounced decrease in the concentrations of other major cations, including Ca, Mg, K and Na.

This enrichment is characterized by a highly homogeneous spatial distribution in the internal structure of the entire zeolite. Figure 12 illustrates the spatial correlation between iron and other elements in zeolite fragments analysed by EDS in TEM, confirming that iron is uniformly incorporated into the structure and proving that effective cation exchange occurred.

BIZ after batch tests

No visible evidence for the precipitation of a stable Cr(III) phase was observed by SEM or TEM. Nevertheless, XRF spectroscopy analysis revealed a significant increase in chromium content after the batch experiments. Unlike TIZ, chromium precipitates are not concentrated on the surface of BIZ grains. Given

https://doi.org/10.1180/clm.2026.10041 Published online by Cambridge University Press

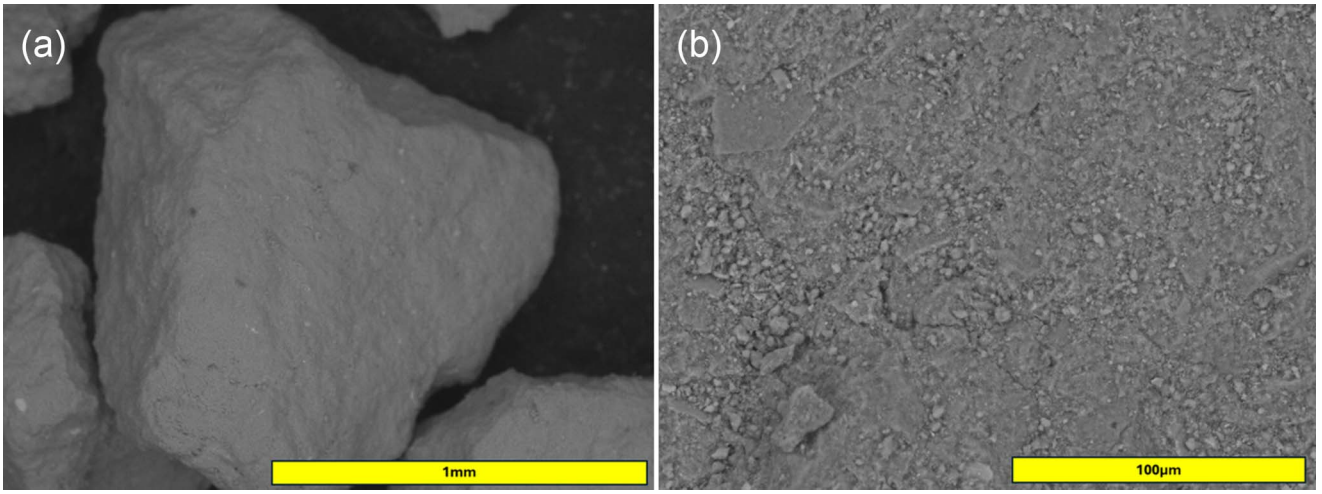


Figure 9. (a) NZ grain sample under SEM with a back-scattered electron (BSE) detector (100×). (b) NZ external surface details at 800× amplification (BSE detector).

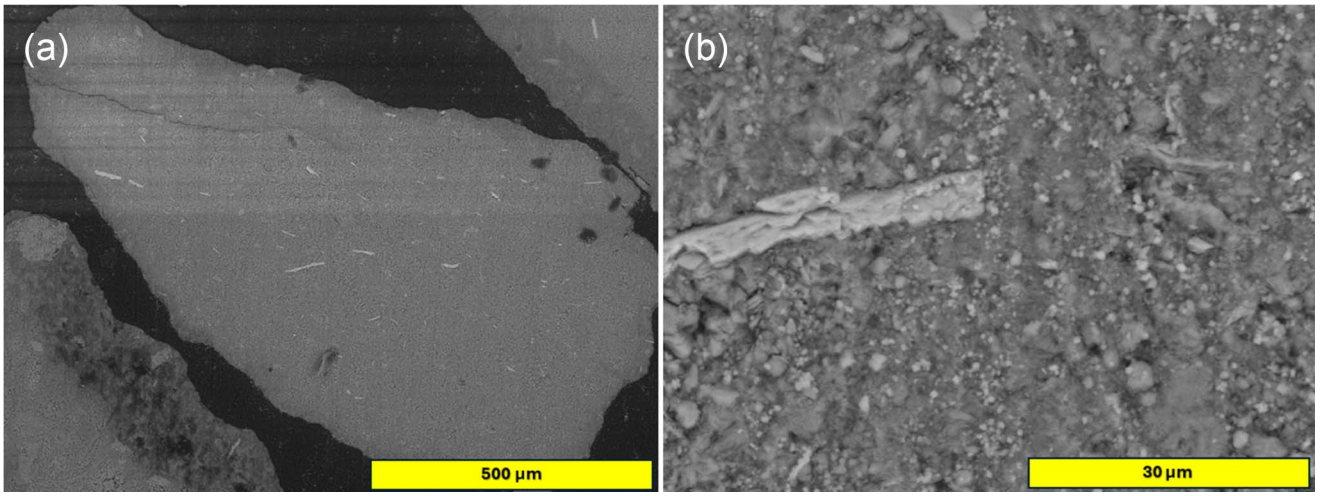


Figure 10. (a) Resin-embedded NZ sample showing its internal structure. (b) 2500× magnification of the clinoptilolite matrix, highlighting its heterogeneity in density and coherence. An elongated plagioclase grain is visible on the left side of the image, with lighter contrast.

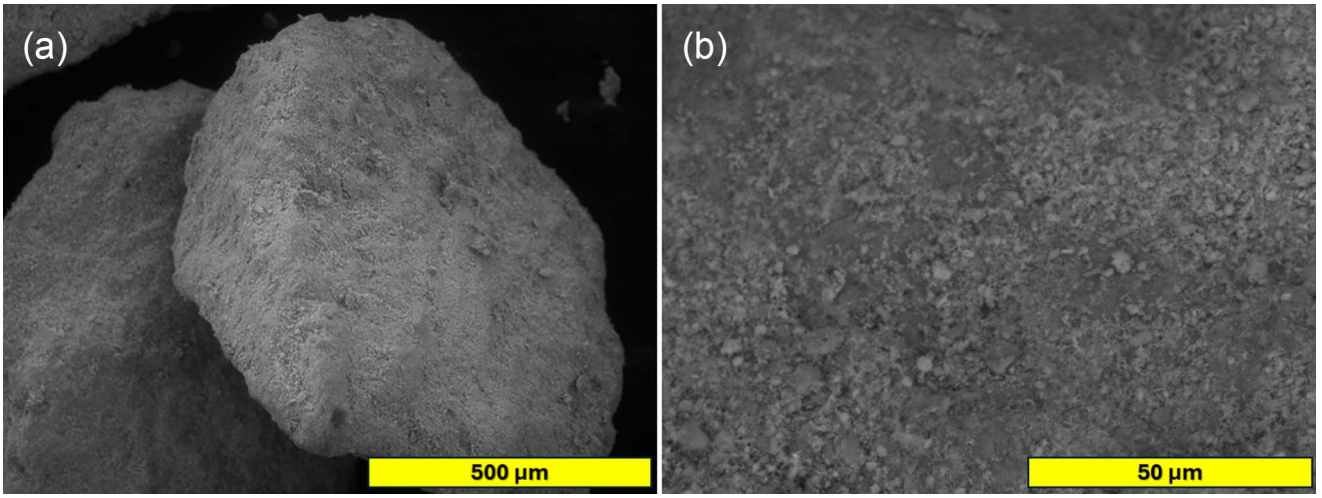


Figure 11. (a) BIZ grain under SEM. (b) 2000× magnification of BIZ's external surface.

https://doi.org/10.1180/clm.2026.10041 Published online by Cambridge University Press

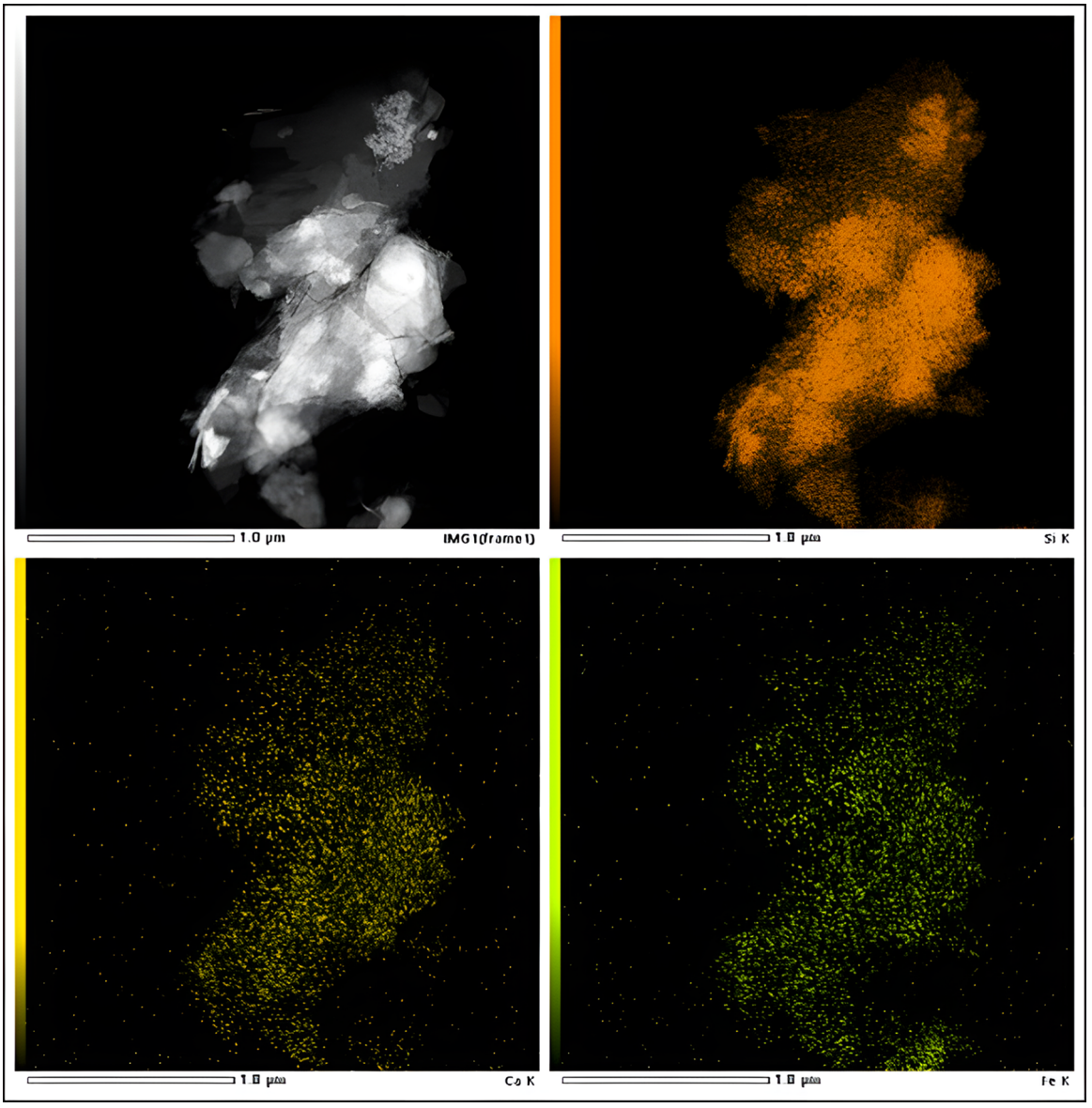


Figure 12. TEM EDS maps from BIZ micro-grains. Top left = scanning TEM image; top left = silicon image; bottom left = calcium image; bottom right = iron image.

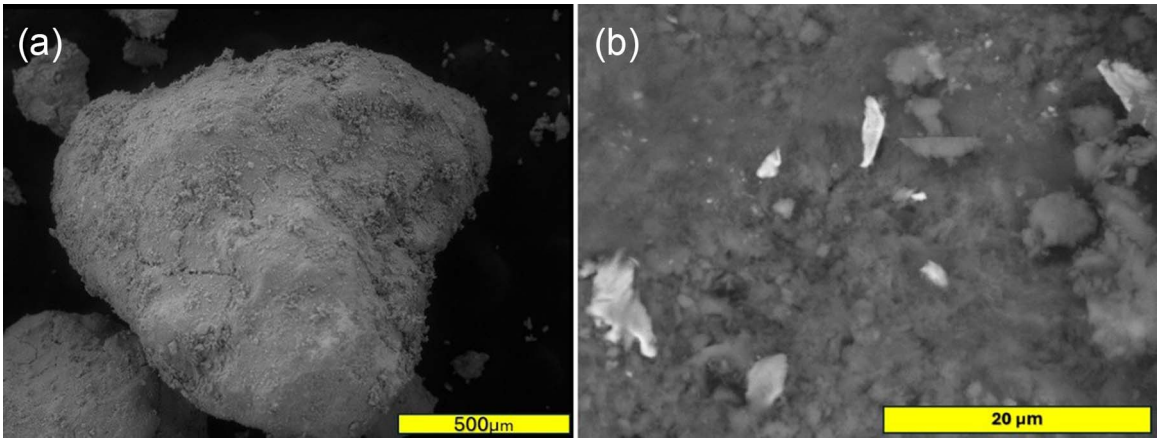


Figure 13. (a) TIZ grain under SEM. (b) 4000× magnification of TIZ's external surface. Small, bright particles are representative of iron oxide/hydroxide phases.

https://doi.org/10.1180/clm.2026.10041 Published online by Cambridge University Press

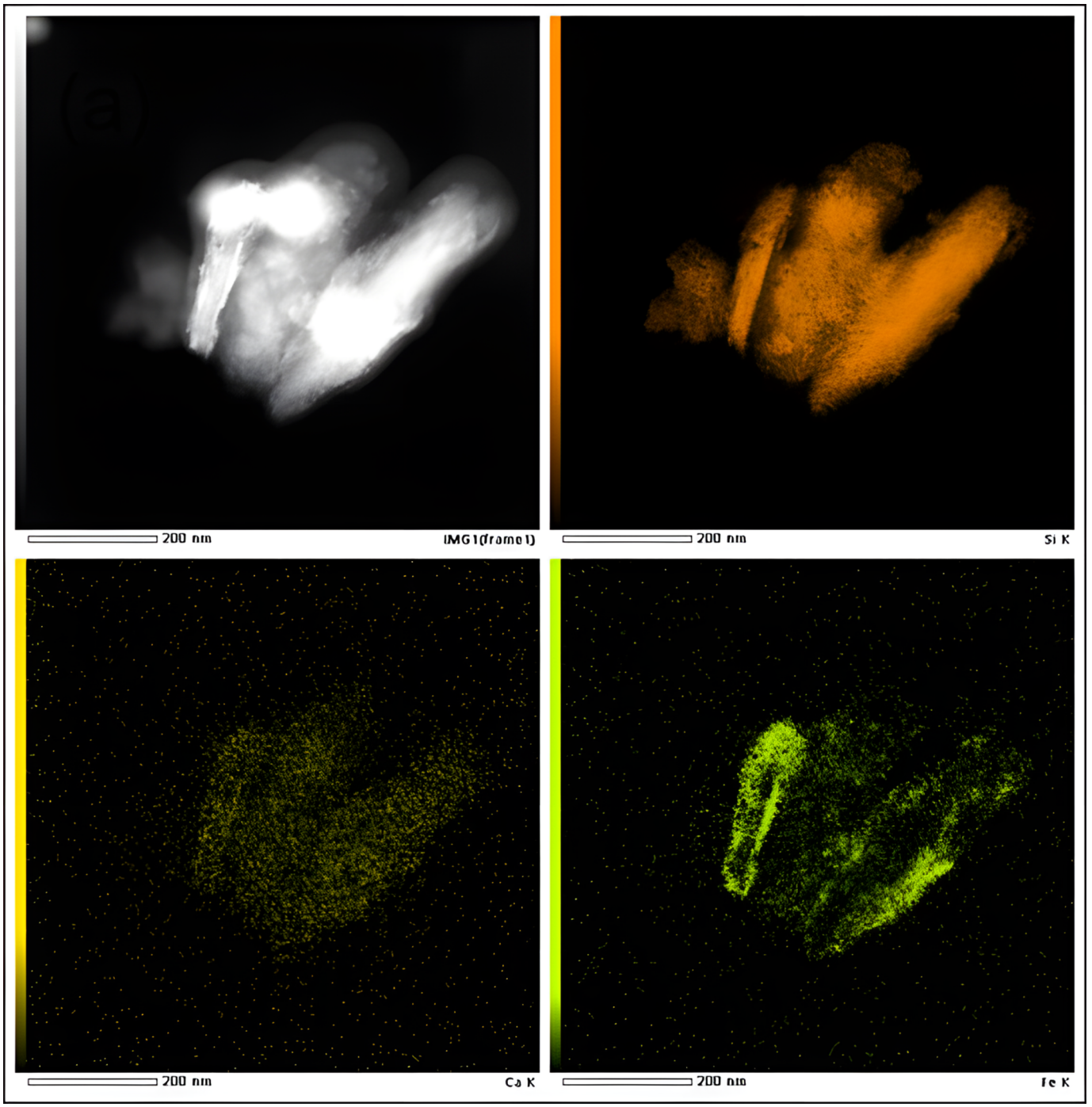


Figure 14. TEM EDS maps from TIZ micro-grains. Top left = scanning TEM image; top right = silicon image; bottom left = calcium image; bottom right = iron image.

the widespread distribution of iron throughout the grains, it is reasonable to assume that the Cr-bearing phases are nanoparticles that are also dispersed within the grain structure. This broad distribution complicates the distinction between true chromium signals and background noise near the detection limits of the analytical method.

Trivalent iron zeolite

The external appearance of TIZ differs significantly from that of NZ. The modification affected not only its chemical composition but also its morphology. The new grains have significantly smoother edges and corners, and the overall grain shape is more rounded than polyhedral (Fig. 13a). At a higher magnification, it is possible to identify various phases covering the surface (Fig. 13b). Bright spots of fine iron oxide particles are frequently dispersed across the surface and vary in size (up to 10 μm). NaCl has also precipitated and is widely distributed throughout the sample.

EDS analysis indicates that the external surface of TIZ grains is highly heterogeneous. The iron distribution varies considerably, and notable increases in chloride and sodium are also observed. No significant chromium concentrations were detected within the

https://doi.org/10.1180/clm.2026.10041 Published online by Cambridge University Press

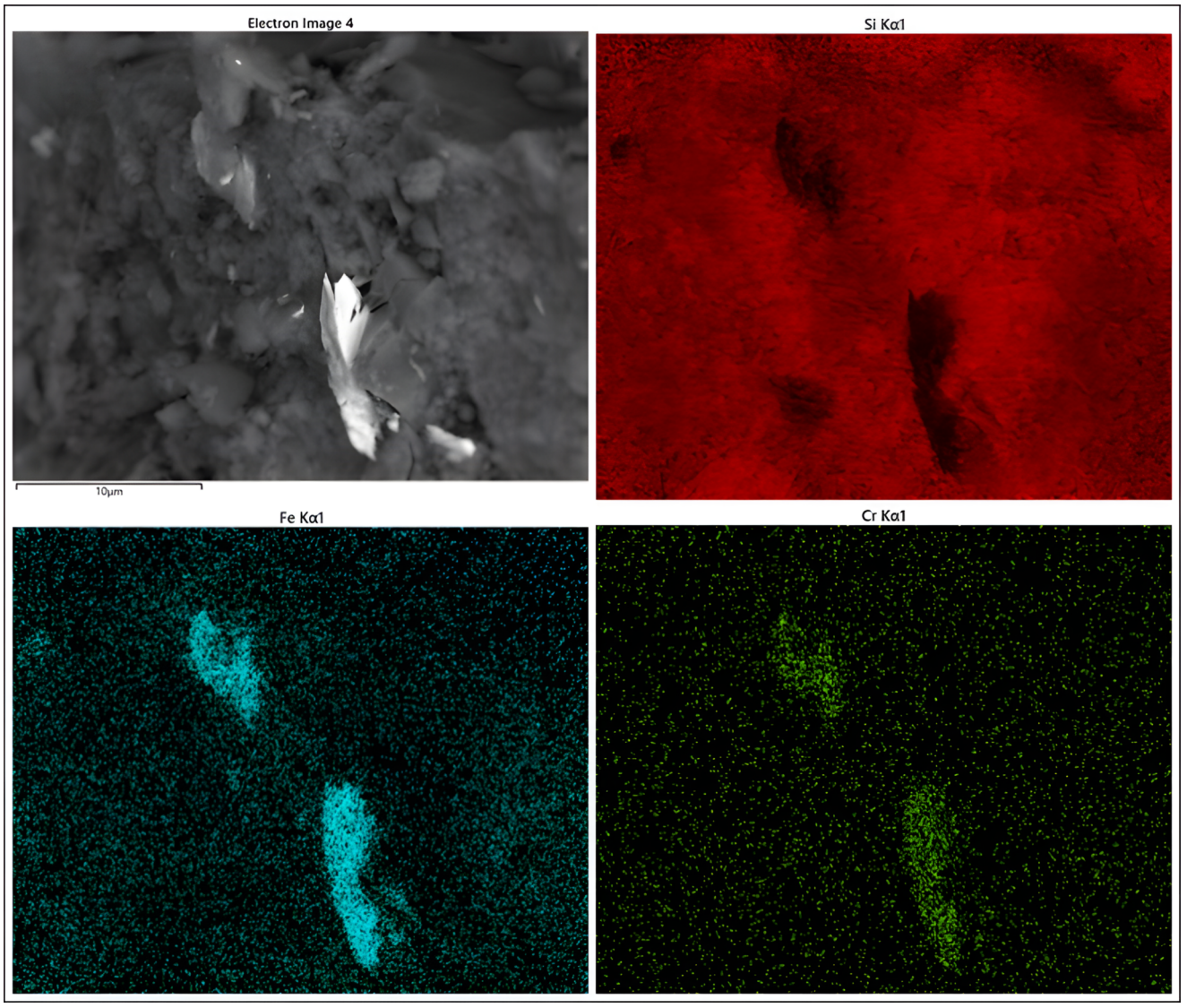


Figure 15. TIZ after Cr(VI) adsorption. (Top left) SEM image with a back-scattered electron detector of the grain surface. (Top right) Silicon EDS map in red. (Bottom left) Tron EDS map in blue. (Bottom right) Chromium EDS map in green.

grains or in association with the iron phases. In contrast, the internal matrix of TIZ shows no substantial alteration relative to NZ, except in larger fractions connected to the external surface, confirming that the chemical modification is largely confined to the grain exterior.

EDS maps of the micro-grains also show a heterogeneous spatial distribution of iron at the nanoscale. Figure 14 illustrates the spatial distribution of elements in the microstructure of TIZ. In contrast to BIZ, iron in TIZ tends to concentrate in specific areas around the main grain.

TIZ after batch tests

Samples of TIZ, after Cr(VI) adsorption, were carefully analysed. Chromium was not detected except in association with iron oxides/hydroxides on the TIZ surface. EDS analysis of the bright particles revealed an average of 53.24 at.% iron and 7.40 at.% chromium. The EDS elemental maps clearly show a strong spatial correlation between these two elements (Fig. 15). The size of the iron oxide/hydroxide crystals varies significantly. Microcrystals up to 10 µm are observable in the SEM images, while nanocrystals were identified through TEM images. These nanocrystals appear to exhibit greater chromium concentrations (up to 18.3 at.%) compared to the larger microcrystals.

Conclusion

NZs are generally considered unsuitable for anion adsorption; however, chemical modification can substantially improve their performance with regards to removing contaminants such as Cr(VI). In this study, two different iron-modified zeolites – BIZ and TIZ – were comparatively evaluated to assess how various modification strategies influence chromium removal mechanisms and efficiency.

The Fe(II)-enrichment procedure used to produce BIZ proved effective at introducing iron to extra-framework zeolite sites through cation exchange, resulting in a homogeneous distribution of Fe(II) throughout the grains. However, some methodological adjustments are recommended to prevent excess reagents from

https://doi.org/10.1180/clm.2026.10041 Published online by Cambridge University Press

impregnating the external surfaces of the grains. BIZ exhibits a higher adsorption capacity (Q), which increases in the presence of other cations and is optimal under mildly acidic conditions. This improved performance is probably linked to its mechanism of reducing Cr(VI) to Cr(III), as confirmed by the isotopic analysis. However, this reduction process in BIZ necessitates a longer contact time because it exhibits slower kinetics. This feature reduces its efficiency in column experiments with synthetic solutions.

In contrast, TIZ modification successfully generated iron oxide/hydroxide phases on the external surfaces of the zeolite grains, which acted as adsorption sites for chromate species. This material exhibits rapid Cr(VI) uptake and reaches adsorption equilibrium within shorter contact times. Following Cr(VI) adsorption, the direct spatial correlation between iron and chromium observed in the EDS maps strongly suggests that direct adsorption is the primary mechanism for removing the target contaminant. Adsorption is best described by the Freundlich isotherm, indicating heterogeneous multilayer sorption on Fe(III) surface phases. Nevertheless, a significant drawback of this material is its high sensitivity to competing anions, which severely limits its applicability in complex water matrices and reduces its effectiveness in the presence of multiple contaminants.

These differing characteristics observed between both modified zeolites do not designate one as inherently superior or inferior to the other; rather, they represent crucial aspects for considering their applicability in diverse scenarios. For instance, when addressing circumstances necessitating the rapid removal of Cr(VI), as can be encountered in industrial filtration systems, with limited contact times between pollutants and zeolites, TIZ emerges as the prime choice due to its rapid adsorption kinetics and efficiency over shorter exposure periods, so long as other competitor anions are not significantly present. Conversely, in contexts where the aim is to achieve a higher adsorption capacity and time constraints are not critical, such as remediating contaminated aquifers with permeable adsorption barriers, BIZ appears to be a more suitable candidate.

Competing interests. The authors declare none.

References

Aharchaou I., Maul A., Pons M.N., Pauly D., Poirot H., Flayac J. *et al.* (2022) Effects and bioaccumulation of Cr(III), Cr(VI) and their mixture in the freshwater mussel *Corbicula fluminea*. *Chemosphere*, **297**, 134090.

Ajouyed O., Hurel C., Ammari M., Allal L.B. & Marmier N. (2010) Sorption of Cr(VI) onto natural iron and aluminum (oxy)hydroxides: effects of pH, ionic strength and initial concentration. *Journal of Hazardous Materials*, **174**, 616–622.

Bish D.L. & Post J.E. (1993) Quantitative mineralogical analysis using the Rietveld full-pattern fitting method. *American Mineralogist*, **78**, 932–940.

Bols M.L., Devos J., Rhoda H.M., Plessers D., Solomon E.I., Schoonheydt R.A. *et al.* (2021) Selective formation of α-Fe(II) sites on Fe–zeolites through one-pot synthesis. *Journal of the American Chemical Society*, **143**, 16243–16255.

Brigatti M.F., Lugli C., Cibin G., Marcelli A., Giuli G., Paris E. *et al.* (2000) Reduction and sorption of chromium by Fe(II)-bearing phyllosilicates: chemical treatments and X-ray absorption spectroscopy (XAS) studies. *Clays and Clay Minerals*, **48**, 272–281.

Chmielewská E., Tylus W., Drábik M., Majzlan J., Kravčak J., Williams C. *et al.* (2017) Structure investigation of nano-FeO(OH) modified clinoptilolite tuff for antimony removal. *Microporous and Mesoporous Materials*, **248**, 222–233.

Coelho A. (2018) *TOPAS* and *TOPAS-Academic*: an optimization program integrating computer algebra and crystallographic objects written in *C++*. *Journal of Applied Crystallography*, **51**, 210–218.

Døssing L.N., Dideriksen K., Stipp S.L.S. & Frei R. (2011) Reduction of hexavalent chromium by ferrous iron: a process of chromium isotope fractionation and its relevance to natural environments. *Chemical Geology*, **285**, 157–166.

Du G., Li Z., Liao L., Hanson R., Leick S., Hoeppner N. & Jiang W.T. (2012) Cr(VI) retention and transport through Fe(III)-coated natural zeolite. *Journal of Hazardous Materials*, **221**, 118–123.

Ellis A., Johnson T. & Bullen T. (2002) Chromium isotopes and the fate of hexavalent chromium in the environment. *Science (New York, N.Y.)*, **295**, 2060–2062.

Franus M., Wdowin M. & Bandura L. (2015) Removal of environmental pollutions using zeolites from fly ash: a review. *Fresenius Environmental Bulletin*, **24**, 854–866.

Gates-Rector S. & Blanton T. (2019) The Powder Diffraction File: a quality materials characterization database. *Powder Diffraction*, **34**, 1–9.

Ghezzi L., Arrighi S., Mugnaioli E., Perchiazzi N., Zamponi E., Pollastri S. *et al.* (2024) Environmental impacts and risk assessment in the re-use of Cr-bearing pyrolyzed tannery wastes: a case study in a residential area. *Applied Geochemistry*, **168**, 106029.

Hao Y., Ma H., Wang Q., Zhu C. & He A. (2022) Complexation behaviour and removal of organic–Cr(III) complexes from the environment: a review. *Ecotoxicology and Environmental Safety*, **240**, 113676.

Hossini H., Shafie B., Niri A.D., Nazari M., Esfahlan A.J., Ahmadpour M. *et al.* (2022) A comprehensive review on human health effects of chromium: insights on induced toxicity. *Environmental Science and Pollution Research International*, **29**, 70686–70705.

Irshad M.A., Sattar S., Nawaz R., Al-Hussain S.A., Rizwan M., Bukhari A. *et al.* (2023) Enhancing chromium removal and recovery from industrial wastewater using sustainable and efficient nanomaterial: a review. *Ecotoxicology and Environmental Safety*, **263**, 115231.

Kiser J. & Manning B. (2009) Reduction and immobilization of chromium(VI) by iron(II)-treated faujasite. *Journal of Hazardous Materials*, **174**, 167–174.

Kitchen J.W., Johnson T.M., Bullen T.D., Zhu J. & Raddatz A. (2012) Chromium isotope fractionation factors for reduction of Cr(VI) by aqueous Fe(II) and organic molecules. *Geochimica et Cosmochimica Acta*, **89**, 190–201.

Kotaś J. & Stasicka Z. (2000) Chromium occurrence in the environment and methods of its speciation. *Environmental Pollution*, **107**, 263–283.

Kwak S., Yoo J.C., Moon D.H. & Baek K. (2018) Role of clay minerals on reduction of Cr(VI). *Geoderma*, **312**, 1–5.

Li Y., Huang Y., Li Z., Tang X., Liu X. & Hughes S.S. (2022) Mechanisms of chromium isotope fractionation and the applications in the environment. *Ecotoxicology and Environmental Safety*, **242**, 113948.

Liu Y., Li H., Tan G.Q. & Zhu X. (2010) Fe^{2+}-modified vermiculite for the removal of chromium(VI) from aqueous solution. *Separation Science and Technology*, **46**, 290–299.

Lofù A., Mastrorilli P., Dell'Anna M.M., Mali M., Sisto R. & Vignola R. (2016) Iron(II) modidied natural zeolite for hexavalent chromium removal from contaminated water. *Archives of Environmental Protection*, ***42***, 35–40.

Lv G., Li Z., Jiang W.T., Ackley C., Fenske N. & Demarco N. (2014) Removal of Cr(VI) from water using Fe(II)-modified natural zeolite. *Chemical Engineering Research and Design*, **92**, 384–390.

Magar V., Martello L., Southworth B., Fuchsman P., Sorensen M. & Wenning R. (2008) Geochemical stability of chromium in sediments from the lower Hackensack River, New Jersey. *Science of the Total Environment*, **394**, 103–111.

Mandiwana K.L., Panichev N., Kataeva M. & Siebert S. (2007) The solubility of Cr(III) and Cr(VI) compounds in soil and their availability to plants. *Journal of Hazardous Materials*, **147**, 540–545.

Martello L., Fuchsman P., Sorensen M., Magar V. & Wenning R. (2007) Chromium geochemistry and bioaccumulation in sediments from the lower

https://doi.org/10.1180/clm.2026.10041 Published online by Cambridge University Press

Hackensack River, New Jersey. *Archives of Environmental Contamination and Toxicology*, **53**, 337–350.

Mortada W.I., El-Naggar A., Mosa A., Palansooriya K.N., Yousaf B., Tang R. *et al.* (2023) Biogeochemical behaviour and toxicology of chromium in the soil–water–human nexus: a review. *Chemosphere*, **331**, 138804.

Munthali M., Elsheikh M., Johan E. & Matsue N. (2014) Proton adsorption selectivity of zeolites in aqueous media: effect of Si/Al ratio of zeolites. *Molecules (Basel, Switzerland)*, **19**, 20468–20481.

Pontér S., Pallavicini N., Engström E., Baxter D. & Rodushkin I. (2016) Chromium isotope ratio measurements in environmental matrices by MC-ICP-MS. *Journal of Analytical Atomic Spectrometry*, **31**, 145A.

Rai D., Eary L.E. & Zachara J.M. (1989) Environmental chemistry of chromium. *Science of the Total Environment*, **86**, 15–23.

Richard F.C. & Bourg A.C.M. (1991) Aqueous geochemistry of chromium: a review. *Water Research*, **25**, 807–816.

Rosa M.I.G., Boga G.A., Cruz S., Furquim S. & Shinzato M.C. (2022) Mechanisms of chromium(VI) removal from solution by zeolite and vermiculite modified with iron(II). *Environmental Science and Pollution Research*, **33**, 49724–49738.

Salem F.Y., Parkerton T.F., Lewis R.V., Huang J.H. & Dickson K.L. (1989) Kinetics of chromium transformations in the environment. *Science of the Total Environment*, **86**, 25–41.

Suhartana, Sukmasari E. & Azmiyawati C. (2018) Modification of natural zeolite with Fe(III) and its application as adsorbent chloride and carbonate ions. *Materials Science and Engineering*, **349**, 012075.

Sultana, Q., Naeem, A., Mahmood, T., Ud Din, I., Saeed, T., Khan, N. & Ahmad, T. (2021) Sorption studies of chromate by iron oxide from drinking water. *Zeitschrift für Physikalische Chemie*, **235**, 407–425.

Sumari, Fajaroh F., Santoso A. & Wardani R.K. (2018) Performance of activated natural zeolite/Cu as a catalyst on degradation of glycerol into ethanol assisted by ultrasonic. *Journal of Physics: Conference Series*, **1093**, 012036.

Tashauoei H.R., Attar H., Kamali M., Amin M. & Nikaeen M. (2010) Removal of hexavalent chromium(VI) from aqueous solutions using surface-modified nanozeolite A. *International Journal of Environmental Research*, **4**, 491–500.

Tumolo M., Ancona V., De Paola D., Losacco D., Campanale C., Massarelli C. & Uricchio V.F. (2020) Chromium pollution in European water, sources, health risk, and remediation strategies: an overview. *International Journal of Environmental Research and Public Health*, **17**, 5438.

Tzou Y., Wang M. & Loeppert R. (2003) Sorption of phosphate and Cr(VI) by Fe(III) and Cr(III) hydroxides. *Archives of Environmental Contamination and Toxicology*, **44**, 445–453.

Unceta N., Séby F., Malherbe J. & Donard O. (2010) Chromium speciation in solid matrices and regulation: a review. *Analytical and Bioanalytical Chemistry*, **397**, 1097–1111.

Vaiopoulou E. & Gikas P. (2020) Regulations for chromium emissions to the aquatic environment in Europe and elsewhere. *Chemosphere*, **254**, 126876.

Villalobos M., Trotz M. & Leckie J. (2001) Surface complexation modeling of carbonate effects on the adsorption of Cr(VI), Pb(II) and U(VI) on goethite. *Environmental Science and Technology*, **35**, 3849–3856.

Young R.A. (1993) The Rietveld method. *Crystal Research and Technology*, **30**, 494–494.

Yu X.Z. & Zhang X.H. (2014) Kinetics for adsorptive removal of chromium(VI) from aqueous solutions by ferri hydroxide/oxohydroxides. *Ecotoxicology*, **23**, 734–741.

https://doi.org/10.1180/clm.2026.10041 Published online by Cambridge University Press